Jian Chong Wei, Yue Ming Gao, Guo Qing Li, Zhi Jiong Wang, Mang I Vai, Peng Un Mak, Min Du and Sio Hang Pun

A Lateral Flow Immunochromatographic Assay (LFIA) Strip Reader Based on Scheduler and 8051 IP Core

Lateral flow immunochromatographic assay (LFIA) testing is essential for accurate detection and diagnoses of diseases and physical conditions. However, the existing LFIA strip reader equipped with high cost of hardware confines its simplicity and portability. Therefore, this study develops a simple, low cost LFIA strip reader comprising 4 major modules — mechanical, optical, processing and control modules. The mechanical module pulls in and out the test strip automatically to be read by the optical module and the data processing module provides the test results by analyzing the data sent by the optical module. All the individual modules are controlled by a control module. To reduce the hardware budget and control complexity, a time-triggered cooperative (TTC) scheduler implemented on an 8051 IP core was chosen as control system. In addition, special, high sensitivity C- reactive protein (CRP) strips with 10 different concentrations were tested to evaluate the performance of the system. Further, a commercial ESEQuant lateral flow reader (QIAGEN, Germany) was tested as a comparative study. The test results show that the proposed reader was stable with a coefficient of variation (CV) factor within 3%. To test the qualitative performance of the system, each of the CRP concentration were examined for 10 times, which indicates that the system has a large dynamic detection range and good detection linearity (R^2 = 0.998). In short, the proposed LFIA strip reader has high potential relative to existing readers, especially in simplicity and cost.

Key words: Lateral flow immunochromatographic assay (LFIA), Strip reader, Scheduler, 8051 IP Core.

Imunokromatografsko testiranje lateralnog toka (LFIA) čitača trake temeljeno na rasporedu i 8051 IP jezgri. Imunokromatografsko testiranje lateralnog toka (LFIA) nužno je za preciznu detekciju i dijagnozu obol-jenja te psihičkih stanja. Međutim, postojeći LFIA opremljeni s hardverom visoke cijene limitiraju jednostavnost i prenosivost. Ovo istraživanje razvija jednostavni, niske cijene, čitač traka koji se sastoji od 4 glavna dijela — mehanički, optički, procesni i upravljački. Mehanički modul povlači testnu traku automatski kako bi optički modul mogao čitati. Procesni modul analizira podatke dobivene s optičkog čitača. Svaki modula upravlja se upravljačkim modulom. Vremensko ovisno kooperativni raspored implementiran je na 8051 IP jezgri kako bi se smanjili računski zahtjevi. Dodatno, visoko osjetljiva CRP traka s deset različitih koncentracija korištena je u svrhe evaluacije sus-tava. Rezultati su uspoređeni s komercijalnim čitačem lateralnog toka ESEQuant (QIAGEN, Njemačka). Rezultati pokazuju da je predložena metoda stabilna s koeficijentom varijacije unutar 3%. Kako bi se kvalitativno testirao sustav, svaka od CRP koncentracija testirana je deset puta, što ukazuje da sustav veliki dinamički raspon detek-cije te dobru linearnost detekcije (R^2 = 0.998). Predloženi LFIA čitač traka ima dosta potencijala u usporedbi s postojećim čitačima, posebno u smislu jednostavnosti i cijene.

Ključne riječi: imunokromatografsko testiranje lateralnog toka (LFIA), čitač traka, raspoređivač, 8051 IP jezgra

1 INTRODUCTION

Lateral flow immunochromatographic assay (LFIA) testing has been used for some time for its several benefits, such as a user-friendly format, long-term stability, and relatively low cost. Therefore, several researchers have studied different aspects of LFIA, such as, specific application areas (tests on drugs, hormones, food, pregnancy, and so on), attractive features (high sensitivity and selectivity) and operational complexity (ease of use) [1-4]. However, most of the systems involved very complicated hardware which increases their cost. Besides, reducing hardware burden of the LFIA detection system has not been thoroughly investigated. In this view, this work aims to develop a simple and low budget LFIA strip reader without compromising any detection efficiency factors – detection time, stability, sensitivity, etc.

As per literature, based on the operating principles and the pertinent system hardware, all LFIA systems

can be categorized into two groups – CCD (charged-couple device) or CMOS (complementary metal-oxide-semiconductor transistor) based imaging system and scanning system [5-8]. The CCD based systems include an image capture unit (camera or image scanner), and an image processing unit (computer or embedded computer). It captures an image of the whole test strip by the image capture unit and performs a specific image processing algorithm to achieve the results. In a CCD based system, the computational complexity is very high because the overall performance of the system depends on the quality of the acquired image. Therefore, a large number of data points are captured by the CCD camera, which requires a highly efficient computer to accomplish the appropriate image processing. Also, the performance of the image processing algorithm has a great impact on the detection accuracy and CCDs are comparatively expensive, which are not suitable for use in a low budget LFIA test reader system [9].

On the other hand, a scanning based system uses a moving unit to scan the test strip and a photodiode for photoelectric conversion. It acquires a 1-D fluorescent distribution signal along the scanning axis. Therefore, signal processing algorithm for the scanning based LFIA reader system is simpler than image processing. Furthermore, it markedly reduces the computational burden and the overall system cost [9]. Gu *et al.* developed a portable fluorescence reader with an S3C2440AL40 (Samsung, Korea) as a main controller and an AT89C51E2 (Atmel, USA) as an auxiliary controller [7]. They focused on finding the best calibration model for quantitative testing without much discussion on hardware burden of the system. Huang *et al.* developed a simple optical reader for lateral flow strip reader, which was controlled by an embedded computer and customized Visual C++ software. In that work, the controlling software was too complex to be implemented in a resource-constrained microprocessor [8]. Certainly, the existing scanning based LFIA strip reader systems are still too complex as they equip with high-level microprocessor and operate in a full RTOS (real time operating system), such as uClinux, which makes the test strip reader more costly and difficulty to transplant to other devices. Therefore, there is an opportunity to reduce the hardware budget of a scanning based LFIA strip reader by incorporating its operations inside a scheduler that can be implemented in a single 8051 chip. It not only reduces the overall system cost but also its complexity.

Eventually, time-triggered cooperative (TTC) scheduler that works as a single timer interrupt service routine can be very suitable for performing the operation of an LFIA strip reader [10, 11]. It is also called a "cyclic executive" because it serves the subroutines in a cyclic manner. The subroutine includes a series of different tasks that should be highly predictable and can be implemented in

resource-constrained systems [12-19]. Indeed, all the individual designated tasks of the scanning based LFIA strip reader are highly predictable and the overall operation can be described as a cyclic manner. Besides, the TTC scheduler facilitates some significant features including high level programming options, very low processor load, and ease of interfacing with new device environment [15]. To run the scheduler, the Oregano System 8051 IP core is very suitable because it includes an optimized processor architecture that offers faster execution than the original 8051 devices. Besides, it embraces with free licensing policy even for the industrial applications, under a LGPL (Lesser General Public License) [20]. Therefore, a TTC scheduler implemented on an 8051 IP Core can offer a simple, low cost, configurable LFIA test strip reader control system, which is consistent with the real time embedded control systems [21].

In this view, this work develops a complete LFIA test strip reader system which includes mechanical, optical and data processing modules. Each of the modules is controlled by a separate central control module. To measure the system performance, high sensitivity C-reactive protein test strips with 10 different concentrations were studied. Further, each test strip was examined 10 times as a repeatability test. In addition, a comparative study was done by testing a commercial ESEQuant lateral flow reader (QIAGEN, Germany).

2   SYSTEM OVERVIEW

An overall systematic block diagram of the LIFA strip reader is shown in Fig. 1, which consists of 4 individual blocks including mechanical, optical, data processing and a control module. According to the instruction provided by the control module, the mechanical module pulls the LFIA test strip in and out by a stepper motor for optical reading. Then, the optical module which consists of an optical unit, an opto-electric unit, and an analog-to-digital (A/D) conversion unit, reads the test strip using UV light. After that, it sends the digital data to data processing module via the control module. The data processing module which is a custom software running on PC, performs specific algorithm for analyzing the test data and displaying the results. The control module (8051 IP core) controls all the operations (detection process) based a prescheduled program.

3   METHODOLOGY

3.1   LFIA strip design

Basically, the LFIA strip consists of 3 sections including a sample pad, an analytical membrane and an absorption pad, as diagrammed in Fig. 2 in which the top and the corresponding cross sectional view of the strip has been
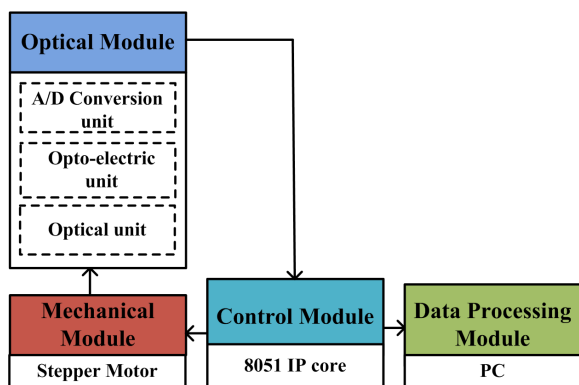
Fig. 1. System overview of the proposed LFIA strip reader system.

Fig. 2. Schematic diagram of a LFIA test strip.

also shown. The sample pad includes an elliptical sample hole through which the test sample is placed drop by drop. After that, the sample flows towards analytical membrane as indicated by arrow. Between the sample pad and analytical membrane, there is a conjugate pad for mobilizing the fluorescent particles, which further helps to quantify the test. The analytical membrane consists of two reaction lines called T-line and C-line, which refers to test line and control line respectively. The T-line indicates the concentration of the test sample and the C-line confirms the validity of the test. Finally, the test sample is absorbed by the absorption pad.

Once the test sample is applied to the membrane, the target antigen (if existed) will be labelled by the fluorescent particles. Then, the induced capillary force draws the conjugate towards the analytical membrane and it reacts with the antibody immobilized there. The targeted biomarker, labelled with fluorescence nanoparticles, anchors in the test lines and exhibits fluorescence corresponding with the concentration of the target antigen. The rest of the chemical within the test sample continue their journey until they reach the absorption pad. This technique, with the induced capillary force, can greatly accelerate the analytical procedures and can simplify the necessary assay procedure for biomarker detection.

The concentration of the biomarkers in the sample can be detected by an optical reading method. The antibody labelled with fluorescent markers and immobilized antibodies in the reaction lines is designed in a way that the light absorbance for a specific wavelength is proportional to the concentration of the biomarkers existed in the sample under test. For instance, an incident light (Φ_i) from a light source can be derived as (1), where Φ_{ss}, Φ_{sf}, and Φ_{af} refer to the amount of light scattered by the testing strip, the amount of light scattered by fluorescent particles, and
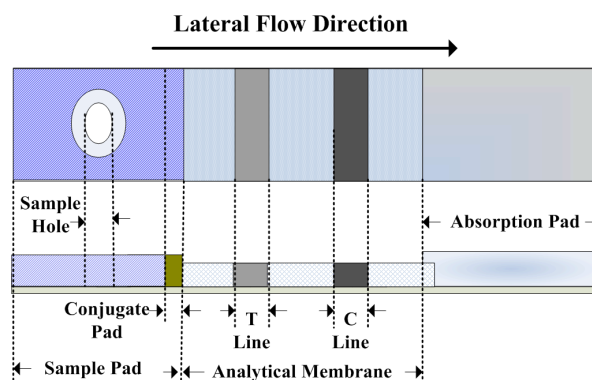
the amount of light absorbed by the fluorescent particles respectively.

$$\Phi_i = \Phi_{ss} + \Phi_{sf} + \Phi_{af}. \tag{1}$$

So the received light (Φ_r) can be derived as,

$$\Phi_r = \Phi_i - \Phi_{af}. \tag{2}$$

Therefore, based on the presence of the number of fluorescent particles in the incident and received light, the concentration of the biomarker in the test sample can be evaluated. However, this requires a very sophisticated optical module which is designed in this work.

3.2   LFIA strip reader system

Stepper motor: The stepper motor controls the actual placement of the LFIA test strips for optical reading by stepwise pulling in and pulling out the platform where the test strips are placed.

Optical unit: As shown in Fig. 3, a sophisticated optical module is used to read the test results from the LFIA test strips. The module includes a UV (ultraviolet) LED, several lenses, and a filter. As shown, there are 2 convex (A and B), a cylindrical lens, and a dichroic lens. Lenses A (vertical) and B (horizontal) are placed in front of the UV LED and the photodiode respectively. Lens A collimates the UV light, which is then reflected by the dichroic lens and passes through the cylindrical lens into the test strip. The dichromic lens is placed at a certain angle to reflect the UV light vertically to the cylindrical lens, which forms the UV light into a line-shaped beam for proper excitation.

The optical module starts its work when the LFIA test strip begins to be pulled in by the stepper motor. First, the LED emits the ultraviolet (UV) light at 365 nm, which gets into the reaction lines of the test strip through lens A,
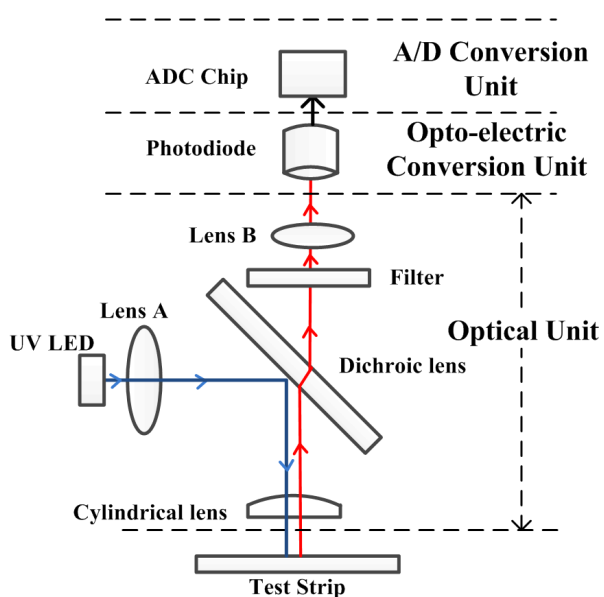
Fig. 3. Configuration of the optical module including optical unit, opto-electric conversion unit, and A/D conversion unit.

dichroic, and cylindrical lenses as indicated by blue line. The strip reemits the light at 610 nm because of the fluorescent particles inside the reaction lines. The light then passes through the dichroic lens, followed by a high pass filter of 580 nm and then lens B as marked by red line.

Opto-electric conversion: The opto-electric conversion unit consists of a photodiode, as shown in Fig. 3. It collects the reflected light and converts into electric signal. Significant variations of the electrical signal can be observed because of variations in the concentration of the test samples.

A/D conversion: The A/D conversion unit converts the analog electrical signal generated by the photodiode to digital signal for further data processing. It includes an ADC chip with a 16-bit resolution, which operates with sample frequency of 250 Hz.

Data processing: The data processing unit runs customized software on PC to analyze the data and show the test results. It collects the digital data from A/D conversion unit via a serial port, and the data transfer scheme is monitored by the control module.

Control module: The control module, called the IP core, controls 3 major tasks: controlling the stepper motor, reading digital data from A/D conversion unit, and transferring data to the data processing module. The IP core is implemented using an 8051 chip, which performs on a Cyclone II FPGA board. Fig. 4 shows the architecture of the control module, which includes a RAM, and an 8051 IP core. The RAM stores the 2 byte data from the A/D conversion unit and transfers it to the data processing module

via a serial port of one byte in two steps. The IP core performs the work based on a TTC scheduler that is described in the next section. In summary, the control module works as follows: First, the stepper motor moves the LFIA strip into the optical module stepwise; next, the data generated by the AD conversion unit is transferred to the RAM; and finally, the data is transferred from the RAM to the data processing module via a serial port. The 3 operations continue in a cyclic way until the whole strip (analytical membrane) is completely scanned.
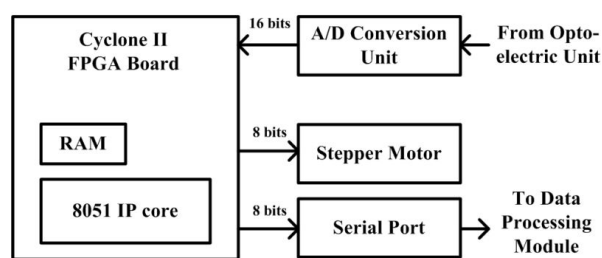
Fig. 4. System architecture of the control module.

4 CONTROL MODULE

The control module was designed based on the scheduler, which is well suited for highly predictable and resource-constrained oriented services. In this view, the time-triggered cooperative (TTC) scheduler was selected to support the LFIA strip test controlling. Before the proposed TTC scheduler operation is explained, the fundamental algorithm of a scheduler is described as follows.

4.1 TTC scheduler algorithm

Generally, the normal operation of the TTC scheduler includes foreground processing and background processing. The foreground processing is in two stages: *Initialization* is performed in three steps: Firstly, a timer is set up to generate scheduler ticks, followed by the initialization of all tasks; next, those tasks are added to the task queue; finally, the scheduled operation is started. During initialization, every task keeps 3 distinct parameters: task name, delay, and period. The task name distinguishes the individual task, delay determines the interval (ticks) before the task is first executed, and period determines the task repeat interval. *Perform task*: This stage includes 3 specific functions: dispatch, cooperative task running, and sleep, which are executed in a loop. The dispatch function determines the task that must be executed from the list. The cooperative task running function executes the tasks that need to run within the tick interval. After that, the sleep function starts to operate, which basically brings the processor into an idle mode to reduce power of the system.

The foreground and background processing algorithms are summarized in Table 1 and Table 2 respectively.

Table 1. TTC scheduler algorithm (foreground processing)

Steps	Remarks
1. Initialization	
1.1: timer set-up	# generate timer interrupt every 1 ms
1.2: add task	# add tasks to the task queue
1.3: start scheduler	# run scheduler
2. Perform task	
Start loop	# while *l*==1
2.1: dispatch	# execute tasks due to run
2.2: task run	# perform tasks
2.3: sleep	# switch processor to idle mode
End loop	

Table 2. TTC scheduler algorithm (background processing)

Steps	Remarks
1: timer ISR	Timer interrupt
2: update	Refresh tasks queue
3: continue with foreground processing	
1: timer ISR	Timer interrupt

4.2   Implementation of TTC scheduler

From the view of the TTC algorithm, the functions of the test strip control system can be divided into three tasks: stepper motor control, AD control, and serial port control (or UART). In implementing the TTC architecture, the most important problem is to estimate the execution time of each task. This is because, as per the fundamental principle of the TTC algorithm, the task time must be highly predictable; i.e., a particular task should complete its execution within the WCET (worst-case execution time), otherwise an overrun situation could arise, which could hamper the overall system performance by introducing the jitters problem [13]. To avoid the jitter problem, the total execution time of all the tasks must be less than one tick.

The cooperative operation of the proposed design is diagrammed in Fig. 5, in which the horizontal direction refers to time in milliseconds and three distinct operations are indicated by P, Q, and R (blue, red, and yellow respectively). Tasks P, Q, and R correspond to 'increase one motor step', 'transfer 2 bytes data from A/D to RAM of the IP Core', and 'transfer 1 byte data through UART from RAM to PC'. As is shown, the operations execute cyclically. From the start of one P to the start of the next P is called the major cycle (t_{maj}), which includes four minor cycles (t_{min}) as displayed; t_{min} = 1 ms and $t_{maj} = 4t_{min}$
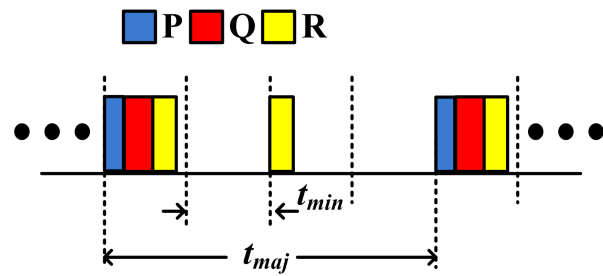
Fig. 5. Cooperative execution of three tasks. P, Q, R represent motor task, AD task, UART task.

= 4 ms based on the required time to do the A/D conversion, where the sampling frequency and resolution of A/D chip is 250 Hz and 16 bits respectively.

As soon as the system is turned on, the optical conversion and A/D chip start their operation, even though the test operation has not been started. Therefore, initially, the A/D chip holds some garbage value. However, that garbage value has no effect on the test data, because the detectable lines of the LFIA strip (T and C lines) are near the middle of the analytical membrane (Fig. 2).Then the controller performs the P, Q and R task consecutively within the first minor cycle; t = 1 ms. The UART transfers one byte at a time and requires 1 ms at the baud rate of 9600 bps. Therefore, during t = 1 ms, the data start to be transferred from IP RAM to PC via UART. During t = 3 ms, the second byte of data is sent to PC. In the meantime, the A/D chip makes the AD conversion and holds it in its memory. After 4ms a similar operation continues. One major cycle of the system is summarized in Table 3, in which first column refers to minor cycle number followed by second and third columns denote system involves and operations respectively.

Table 3. System components involved in each minor cycle

Minor cycle (t_{min})	System involves	Operations
1 st	Motor, A/D, IP core, UART	P (increase one motor step), Q (read 2 byte data from AD), R (start transfer 1 byte data via UART)
2 nd	IP core, UART	Continues data transfer via UART
3 rd	IP core, UART	R (start to transfer 1 byte data via UART)
4 th	IP core, UART	Continues data transfer via UART

5 EXPERIMENT

5.1 Test samples

To examine the performances of the LFIA strip reader, C- reactive protein (CRP), which is strongly associated with infections and diseases that cause inflammation [22-25], was used. Therefore, a special, high sensitivity CRP test strip kit was prepared by Triplex International Biosciences Co. Ltd., China. The test strip included CRP antibody (or antigen) immobilized on the test line of the nitrocellulose membrane of the lateral flow strip, and avidin on the control line. For biomarker labelling, a mixture of CRP antibody and biotin-conjugated markers were conjugated with fluorescent particles. The testing was done with different CRP samples of different concentrations in 10 standards between 0.98 μg/mL and 500 μg/mL, including 0.98 μg/mL, 1.95 μg/mL, 3.91 μg/mL, 7.81 μg/mL, 15.6 μg/mL, 31.25 μg/mL, 62.5 μg/mL, 125 μg/mL, 250 μg/mL, and 500 μg/mL. To find the stability of the system, further repeatability test was done 10 times on each strip.

5.2 Experimental steps

First, the samples were prepared in different concentrations and then placed 2 to 3 drops of the sample into the hole of the LFIA strip and wait for 5 to 6 min until the immunochromatographic assay was finished. Then, we inserted the LFIA test strip into the optical module and clicked the Start button on the PC program to begin the detection. During this time, the strip holding platform moved forward along the length axis of the strip, driven by the stepper motor as mentioned. After a certain time (14 s) the strip holding platform returned to its initial position; i.e., the strip detection was finished, and the distribution curve of fluorescence signal displays on the PC monitor. Finally, to start the data processing the Process button was clicked and the final detection results could be observed and analyzed.

5.3 Experimental system

Fig. 6 (a) shows the overall test system and its major components, including data analysis module, central control module, A/D conversion circuit, step motor driver, analog signal processing section, power supply circuit, and optical module. All are indicated by numerical numbers. Further, Fig. 6 (b) displays the major components of the optical module including opto-electric conversion circuit, test strip, opto-sensing module, transmit mechanism, and stepper motor. Some of the important components and their specifications including manufactures are also listed in Table 4.
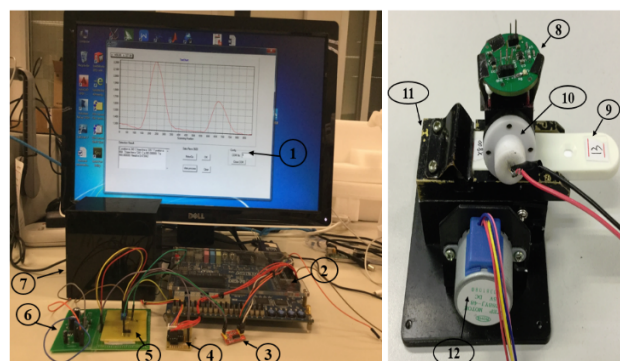
Fig. 6. Overall experimental system (left); Optical module; where, 1: Data processing module, 2: Control module, 3: A/D conversion unit, 4: Stepper motor driver, 5: Analog signal processing section (including signal amplifier, per-conditioning, de-noising circuit), 6: Power supply, 7: Opto-electric unit, 8: Opto-electric conversion unit, 9: LF test strip, 10: Optical unit, 11: Test strip moving parts, 12: Stepper motor (right).

Table 4. Major component of the LFIA system.

Function	Component	Manufacturer
AD conversion	TM7705	Analog Device, Inc. U.S.A.
Drive stepping motor	ULN2003	STMicroelectronics, Korea
Stepping motor	28BYJ-48	Kiatronics, Tauranga, N.Z.
Photoelectric conversion	S1122-14	Hamamatsu, U.S.A.
Analog signal amplify	OPA657	Texas Instrument, U.S.A.
Implement 8051 IP core	Cyclone II	Altera, U.S.A.

6 RESULT AND DISCUSSIONS

6.1 System test

To examine the real operation of the TTC scheduler, a pin high was set in a task running duration and the execution time of every task was analyzed by oscilloscope (MSO7054A, Agilent). As shown in Fig. 7, A, B, C represent motor task, AD task, and UART task respectively. Motor task increased one motor step followed by AD task read 2 bytes data from AD chip. Because UART task sent 1 byte of data at a time, it executed twice to send 2 bytes data. The 3 tasks operated in a cyclic way consistent with the designed operate schedule (Fig. 5). Obviously, the three tasks finished within one tick (t_{min} = 1 ms) and cyclically executed in every major cycle (t_{maj} = 4 ms). Therefore,

the system operated the scheduled detection tasks with no task jitter and over-run.
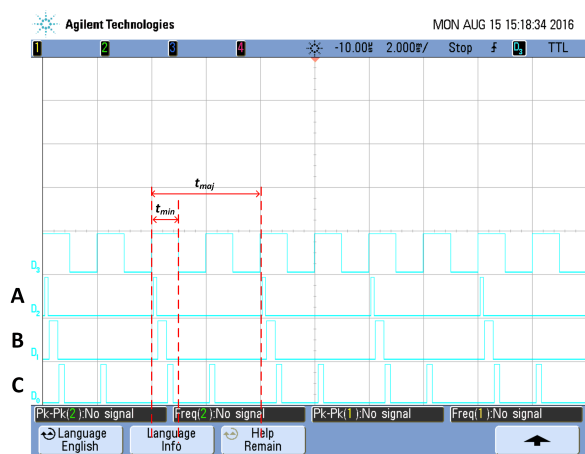
Fig. 7. *Real operation of TTC scheduler, where, A, B, and C represent motor task, AD task, and UART task respectively.*

6.2 Strip test

The acquired data of the fluorescence signal distribution of the test strip collected from the optical module is displayed in Fig. 8, in which the horizontal and vertical axes refer to scanning steps of the stepper motor and amplitude in volt. As shown in Fig. 8(a), the original data were full of burrs and spikes because of high frequency random noise in the circuit. Therefore, a low pass filter was used to remove the noise, and further, a median filter was used to make the signal smoother, as shown in Fig. 8(b). There are 2 high peaks at scanning steps around 460 and 1320, which correspond to T-line (red) and C-line (blue) respectively, and marked by V_T and V_C respectively.

For quantitative detection of LIFA system, 4 calibration models were proposed early on, including ratio of area (ST/SC) with a single baseline, the ratio of area (ST/SC) with variable baseline, the ratio of peak (V_T/V_C) with a single baseline, and the ratio of peak (V_T/V_C) with a variable baseline; where, ST and SC correspond to the area of the test and control lines, and VT and VC correspond to the peak value of the test and control lines separately. Gu *et al.* [7] compared these 4 calibration models and suggested that the ratio of peaks (V_T/V_C) with a variable baseline was the most suitable. Therefore, the ratio of peaks (V_T/V_C) with a variable baseline based calibration model has been considered.

Now, the ratio of 2 peaks (V_T/V_C) with a variable baseline was used for the measured value of an LFIA test strip. Further, to find the repeatability of the results for
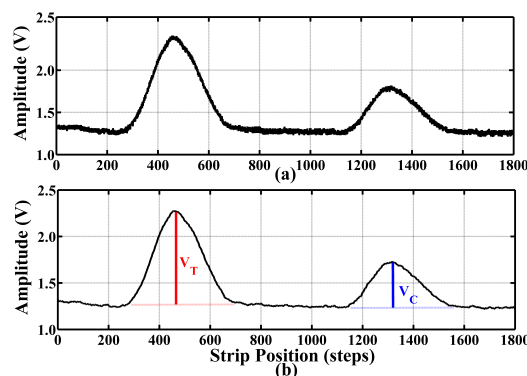
Fig. 8. *(a) Raw test data from optical module. (b) Filtered test data.*

V_T/V_C, each concentration experiment was done for 10 times to calculate the coefficient of variation (CV). Test results are listed in Table 5. The results show that although SD of V_T/V_C slightly increased as concentration rose from 0.98 μg/mL to 250 μg/mL, SD of V_T/V_C were all lower than 0.02. Further, the CV of V_T/V_C in the entire quantitative detection range were all less than 3% except at the lowest concentrations (0.98 μg/mL). Thus, the system performed stable detection. However, it was saturated at 500 μg/mL, which indicates that the reader has large dynamic detection range of sample concentration of 0.98 μg/mL to 250 μg/mL.

Table 5. *Test results of the LFIA strip reader for different concentrations.*

Concentration (μg/mL)	Average V_T/V_C	SD V_T/V_C	CV (%)
0.98	0.02	0.0009	4.50
1.95	0.04	0.0010	2.39
3.91	0.10	0.0013	1.30
7.81	0.19	0.0011	0.55
15.6	0.41	0.0016	0.39
31.25	0.82	0.0033	0.41
62.5	1.53	0.0040	0.26
125	2.90	0.0073	0.25
250	6.33	0.0246	0.39
500	—	—	—

For comparison, an ESEQuant lateral flow reader (QIAGEN, Germany) was tested. Results are shown in Table 6, which indicates that the SD and CV of V_T/V_C were lower than those of test results of the proposed LFIA strip reader. Therefore, ESEQuant has better detection stability at low concentrations. However, it is saturated at 62.50 μg/mL, which indicates that dynamic detection range of ESEQuant is smaller than that of the LFIA strip

reader.

Table 6. Test results of ESEQuant for different concentration.

Concentration (μg/mL)	Average V_T/V_C	SD V_T/V_C	CV (%)
0.98	0.02	0.0006	3.27
1.95	0.05	0.0005	1.09
3.91	0.14	0.0014	0.98
7.81	0.24	0.0012	0.52
15.60	0.49	0.0023	0.46
31.25	0.85	0.0015	0.18
62.50	—	—	—

To analyze the linear detection performance of the system, linearity testing of the test results was done, as shown in Fig. 9, in which the horizontal and vertical direction (both in logarithmic scale at a base of 10) refer to concentration of the test sample and V_T/V_C respectively. As shown, the system performed linearly with a good correlation ($R^2 = 0.998$). The linear analysis of the data indicates a sensitivity of 0.0249 ± 1.45E-4. However, it is notable that the data points slightly deviate from the linear trend at the lowest two concentrations (0.98 μg/mL and 1.95 μg/mL). Therefore, this LFIA strip reader performed stable detection with large dynamic detection range, which shows its potential for reading LFIA strip. However, stability of the system is not as good as ESEQuant lateral flow reader in low concentrations. Besides, the system must be passed through a clinical trial which will be done very soon.

Equation	y = a + b		
Adj. R-Squ	0.99801		
		Value	Standard Er
B	Intercept	-0.012	0.03787
B	Slope	0.0249	3.93578E-4
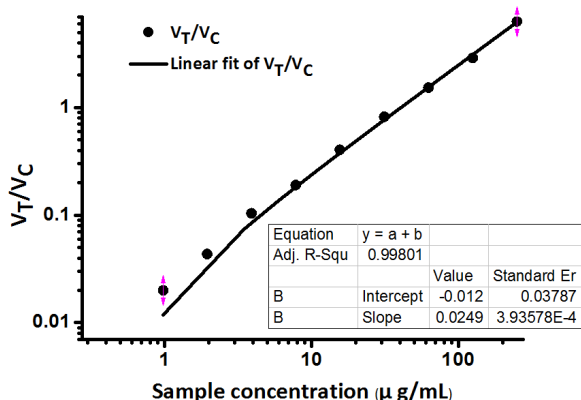
Fig. 9. Linearity of this LFIA strip reader.

7   CONCLUSION

This work describes a lateral flow immunochromatographic assay (LFIA) strip reader which includes four ma-

jor modules: mechanical, optical, data processing and control. The mechanical module pulls the test strip in and out automatically to position it for the optical module. Then the optical module sends the test data via control module to data processing module, which analyses the data and displays the test results. Three of the modules are controlled by a control module that is programmed on an 8051 IP core. In addition, a TTC scheduler is implemented in the 8051 IP core to cyclically control the operations. The IP core works on a FPGA platform (Cyclone-II). The overall performance of the system was tested by the high-sensitivity C-reactive protein (CRP) test strip with 10 different concentrations. The test results show that the system can detect the different CRP concentrations with a CV (coefficient of variation) factor within 3%, which attests to the stability of the system. To evaluate qualitative performance of the system, a repeatability test was done by examining each concentration of the CRP 10 times, which indicates that the system had very good detection linearity ($R^2 = 0.998$). In a comparative study, an ESEQuant lateral flow reader (QIAGEN, Germany) was tested. The results show that ESEQuant had better detection stability in low concentrations, but smaller dynamic detection range than the proposed LFIA strip reader. Thus, the system shows its potential for reading LFIA strip. Besides, the system becomes more effective for its simplicity and easy to use.

REFERENCES

[1] J. R. Reddy, J. Kwang, K. F. Lechtenberg, N. C. Khan, R. B. Prasad, and M. M. Chengappa, "An immunochromatographic serological assay for the diagnosis of Mycobacterium tuberculosis," Comp. Immunol. Microbiol. Infect. Dis., vol. 25, pp. 21–27, 2002.

[2] H. Watanabe, A. Satake, Y. Kido, and A. Tsuji, "Monoclonal-based enzyme-linked immunosorbent assay and immunochromatographic rapid assay for salinomycin," Anal. Chim. Acta, vol. 437, pp. 31-38, 2001.

[3] D. Malamud, H. Bau, S. Niedbala, and P. Corstjens, "Point detection of pathogens in oral samples," Adv. Dent. Res., vol. 18, pp. 12-6, 2005.

[4] J. Hampl, M. Hall, N. A. Mufti, Y. M. M. Yao, D. B. Macqueen, W. H. Wright, et al., "Upconverting Phosphor Reporters in Immunochromatographic Assays ?," Anal. Biochem., vol. 288, pp. 176-87, 2001.

[5] L. G. Lee, E. S. Nordman, M. D. Johnson, and M. F. Oldham, "A low-cost, high-performance system for fluorescence lateral flow assays," Biosensors, vol. 3, pp. 360-373, 2013.

[6] J. J. Li, A. L. Ouellette, L. Giovangrandi, D. E. Cooper, A. J. Ricco, and G. T. Kovacs, "Optical scanner for immunoassays with up-converting phosphorescent labels," IEEE Trans. Biomed. Eng., vol. 55, pp. 1560-1571, 2008.

[7] Y. Gu, Y. Yang, J. Zhang, S. Ge, Z. Tang, and X. Qiu, "POINT-OF-CARE TEST FOR C-REACTIVE PROTEIN BY A FLUORESCENCE-BASED LATERAL FLOW IMMUNOASSAY," Instrum. Sci. Technol., vol. 42, pp. 635-645, 2014.

[8] L. Huang, L. Zhou, Y. Zhang, C. Xie, J. Qu, A. Zeng, et al., "A simple optical reader for upconverting phosphor particles captured on lateral flow strip," IEEE Sens. J., vol. 9, pp. 1185-1191, 2009.

[9] R. C. Wong and H. Y. Tse, Lateral Flow Immunoassay. Totowa, NJ, United States: Hummana Press Inc., 2010.

[10] M. Nahas, "Implementation of highly-predictable time-triggered cooperative scheduler using simple super loop architecture," Int. J. Electr. Comput. Sci., vol. 11, pp. 33-38, 2011.

[11] C. D. Locke, "Software architecture for hard real-time applications: cyclic executives vs. fixed priority executives," Real-Time Syst., vol. 4, pp. 37-53, 1992.

[12] M. Short, "Analysis and redesign of the 'TTC' and 'TTH' schedulers," J. Syst. Archit., vol. 58, pp. 38-47, 2012.

[13] E. Anbarasi, N. Karthik, and R. Prabakaran, "Analysis of time triggered schedulers in embedded system," IEEE 2011 3rd Int. Conf. Electron. Comput. Technol. (ICECT), 2011, pp. 134-137.

[14] A. K. Gendy and M. J. Pont, "Automatically configuring time-triggered schedulers for use with resource-constrained, single-processor embedded systems," IEEE Trans. Ind. Inf., vol. 4, pp. 37-46, 2008.

[15] S. Kuankid, A. Aurasopon, and W. Sa-Ngiamvibool, "Effective scheduling algorithm and scheduler implementation for use with time-triggered co-operative architecture," Elektron. Elektrotech., vol. 20, pp. 122-127, 2014.

[16] M. Short and M. J. Pont, "Fault-tolerant time-triggered communication using CAN," IEEE Trans. Ind. Inf., vol. 3, pp. 131-142, 2007.

[17] S. Kurian and M. J. Pont, "The maintenance and evolution of resource-constrained embedded systems created using design patterns," J. Syst. Software, vol. 80, pp. 32-41, 2007.

[18] T. Phatrapornnant and M. J. Pont, "Reducing jitter in embedded systems employing a time-triggered software architecture and dynamic voltage scaling," IEEE Trans. Comput., vol. 55, pp. 113-124, 2006.

[19] T. Nghiem, G. J. Pappas, R. Alur, and A. Girard, "Time-triggered implementations of dynamic controllers," Proceedings of the 6th ACM & IEEE Int. conf. Embed. soft., 2006, pp. 2-11.

[20] O. System, "MC8051 IP Core User Guide," 2013.

[21] J. Babić, "MODEL-BASED APPROACH TO REAL-TIME EMBEDDED CONTROL SYSTEMS DEVELOPMENT WITH LEGACY COMPONENTS INTEGRATION," 2014.

[22] H. Kuo, C. Yen, C. Chang, C. Kuo, J. C. Chen, and F. A. Sorond, "Relation of C-reactive protein to stroke, cognitive disorders, and depression in the general population: systematic review and meta-analysis," Lancet Neurol., vol. 4, pp. 371-380, 2005.

[23] K. Lin, F. Wang, M. Wu, B. Jiang, W. Kao, H. Chao, et al., "Serum procalcitonin and C-reactive protein levels as markers of bacterial infection in patients with liver cirrhosis: a systematic review and meta-analysis," Diagn. Microbiol. Infect. Dis., vol. 80, pp. 72-78, 2014.

[24] E. T. Yeh, "CRP as a mediator of disease," Circulation, vol. 109, pp. II-11-II-14, 2004.

[25] T. W. Du Clos and C. Mold, "C-reactive protein," Immunol. Res., vol. 30, pp. 261-277, 2004.

Jian Chong Wei received the B.Sc. degree in electronic information engineering from Fuzhou University, Fujian, China. He is currently working toward the M.Sc. degree from the College of Physical and Information Engineering, Fuzhou University, Fujian, China. Since 2014, he has been involved in research in the areas of biomedical engineering.

Yue Ming Gao received the Ph.D. degree in electrical engineering from Fuzhou University, Fuzhou, China, in 2010. Since 2004, he has been involved in research in the areas of bioelectromagnetism and detecting technology. He is currently an Assistant Researcher in the College of Physical and Information Engineering, Fuzhou University.

Zhi-Jiong Wang received the B.Sc. degree in Electronic Science and Technology College of Jilin University in 2014, and the M.Sc. degree from the department of Electrical and Computer Engineering, University of Macau, Macao, China in 2017. He has been with the Biomedical Engineering Lab and State Key Laboratory of Analog and Mixed-signal VLSI as a Research Assistant(2014-2017).His research field are embedded systems and digital VLSI circuits.

Mang I, Vai received his BSc in Physics from Huaqiao University, China, 1984, MSc in Electronics Engineering, Jinan University, China, 1989 and PhD in Electrical and Electronics Engineering from the University of Macau, China, 2002. He is now an Associate Professor and the coordinator of the Biomedical IC Research Line in the State Key Laboratory of Analog & Mixed-Signal VLSI of the University of Macau, and an Associate Professor and the coordinator of the Biomedical Engineering Lab in the Department of Electrical and Computer Engineering of the University of Macau. His current research interests include Biomedical Electronics, Embedded Systems, Neural Engineering and Human Body communication.

Peng Un Mak received the B.Sc. degree in electrical engineering from National Taiwan University, Taipei, Taiwan, and the M.Sc. and Ph.D. degrees in electrical engineering from Michigan State University, East Lansing, Michigan, USA. He has been the first Assistant Professor with the Department of Electrical and Computer Engineering, University of Macau, Macau, Macau SAR, China, since 1997. Authored and/or co-authored over 140 peer-reviewed technical publications (journal, book chapter, and conference proceedings), he has performed research interests in biosignals extraction and processing, bioelectromagnetism, human body communication, and body sensor network. Dr. Mak is also a life member of Phi Kappa Phi and an invited member of Eta Kappa Nu (currently IEEE-HKN).

Sio Hang Pun received his Master degree in Computer and Electrical program from the University of Porto, Portugal, 1999 and the Ph. D Degree in the Electrical and Electronics Engineering from the University of Macau, Macau, 2012. Since 2012, he is an Assistant Professor in the State Key Laboratory of Analog & Mixed-Signal VLSI of the University of Macau. His current research interests include Biomedical Electronic Circuits, Miniaturized Sensors for Biomedical Applications and Human Body communication.

AUTHORS' ADDRESSES

Dr. Yue Ming Gao,
College of Physics and Information Engineering,
Fuzhou University,
Fujian, China,
Email: fzugym@163.com

Mang I Vai,
Dept. of Electrical & Computer Engineering,
Faculty of Science and Technology, University of Macau,
Macau, Macau SAR, China
Email: fstmiv@umac.mo

P. Mak,
Room 3037, Bldg. E11, HengQin (HQ) campus,
Biomedical Engineering Lab.,
Dept. of Electrical & Computer Engineering,
Faculty of Science and Technology, University of Macau,
Macau, Macau SAR,
Email: fstpum@umac.mo

Pun Sio Hang,
Email:lodgepun@umac.mo